

SUPERPLASTIC FORMING BEHAVIOUR OF ALUMINIUM BASED SiC_p REINFORCED METAL MATRIX COMPOSITES

C.M. Styles, N.J. Lindsay and A. Tarrant[†]

SMC, DERA, Farnborough, UK.

[†]Aerospace Metal Composites, RAE Road, Farnborough, UK.

Abstract

Superplastic forming of complex shapes using a single operation and one surface tool is appealing, especially for metal matrix composites (MMCs) that contain hard ceramic reinforcements such as SiC. The current research set out to explore high strain rate superplasticity (HSRS) in aluminium based SiC_p reinforced MMCs aimed at commercial exploitation. Steps were successfully formed in an MMC at high strain rates ($\sim 2 \times 10^{-1} \text{s}^{-1}$). Fine grain size was found to be more important for HSRS, however, large improvements in forming were observed above the matrix solidus where some liquid phase was present.

Keywords

High strain rate superplasticity, Metal matrix composite, Grain size, Liquid phase

Introduction

From a commercial viewpoint superplastic forming of complex shapes using a single operation and one surface tool is appealing, especially for metal matrix composites (MMCs) that contain hard ceramic reinforcements such as SiC. The current research sets out to explore high strain rate superplasticity (HSRS) in aluminium based SiC_p reinforced MMCs aimed at commercial exploitation.

Materials and Experimental

The material used to determine the forming envelope was a 7475 aluminium alloy reinforced with either 17vol% or 10vol% of 3 μm SiC particles. It was manufactured by Aerospace Metal Composites via a powder route and was processed to 0.55mm thickness at DERA, Farnborough.

Samples for optical microscopy were polished to 1 μm ; colloidal silica was employed as a final treatment to improve the matrix appearance. Grain structures were examined by viewing anodised films under polarised light. The unpolished sides of the sample were coated with "Lacomit" varnish prior to anodising in "Barkers" reagent (5ml HBF₄ [50% solution], 200ml H₂O). For optimum anodising conditions, the solution was maintained at $\sim 0^\circ\text{C}$ to reduce surface pitting and a potential of 15V was applied to the sample. When sufficient film had formed the specimen was removed from the electrolyte, washed in water and dried in a stream of air.

Samples of 7475 (17% reinforcement) were formed at 450, 475, 500, 525 and 550 $^\circ\text{C}$ and forming pressures of 100, 200 and 300psi. The 7475 (10% reinforcement) material was formed at 450 $^\circ\text{C}$ /300psi and 550 $^\circ\text{C}$ /200psi. The die mould had a 45 $^\circ$ step which it was hoped the MMC would

form around. The gas pressure was applied for twenty seconds or until the material burst in the unrestrained region behind the die. After forming the angle of the step was measured in accordance with Figure 1 and materials were sectioned through the step and polished to look for cavitation. Strain rates of forming were determined by applying the forming pressure for a set amount of time. Differential scanning calorimetry was performed at a heating rate of 2°C/min to determine the matrix solidus. Fracture surfaces above and below the matrix solidus were observed in a scanning electron microscope to look for filaments which are indicative of a liquid phase being present.

Results

Anodised films viewed under polarised light showed up the grain structures of the 7475 MMC with 10 and 17% reinforcement. It was seen that there was some directionality of grain structure and grain sizes of the 17vol% material were 2-3µm and the 10vol% material were ~7x15µm.

From Figure 2 it can be seen that steps formed in the 7475 (17vol%) MMC across the range of temperatures. Table I shows the forming properties of this material; quoted angles are α from Figure 1. It can be seen that the angles formed range from 22° to 42° and higher pressures are required at the lower temperatures. Figure 3 shows the forming envelope of this material with step angle plotted as a function of temperature.

Table I. Step angles for the 7475 (17vol%) material

	100psi	200psi	300psi
450°C	N	N	22°
475°C	--	22°	--
500°C	N	27°	31°
525°C	N	30°	36°
550°C	35°	42°	X

N = did not form

X = could not reach this pressure as unrestrained material burst at 200psi

Figure 4 shows 7475 (10% reinforcement) formed at 525°C/300psi and 550°C/200psi. It can be seen that the material has not formed a step but has split. The split appears to emanate from the stress concentration at the step.

DSC heating and cooling curves for the MMCs showed the onset of melting appears to be at 540°C and freezing at 530°C. Due to measuring lags the matrix solidus can be estimated as 535°C.

Figure 5 shows the polished section through the step region of the 7475 (17vol%) MMC formed at 550°C/200psi. It can be seen that no matrix cavitation, particle matrix debonding or SiC particle fracture has occurred. This was found to be the case for this material at all forming temperatures and pressures.

The fracture surface for the 7475 (17vol%) MMC formed at 550°C is shown in Figure 6. At 550°C thread like filaments were seen and some evidence of smearing. This was not the case for the material formed at 525°C below the matrix solidus.

Discussion

Strain rates were measured in a large die that allowed up to 70% strain. At 550°C/200psi the strain rate measured was $\sim 2 \times 10^{-1} \text{s}^{-1}$ and at 500°C/200psi $\sim 1.4 \times 10^{-1} \text{s}^{-1}$ for the 7475 (17% reinforcement) MMC. It is generally accepted that HSRS is exhibited at strain rates $> 10^{-2} \text{s}^{-1}$. At the highest strain rate 70% strain was achieved in only 3.5 seconds which is very attractive for commercial exploitation.

High strain rate superplasticity was first shown in 1984 by Nieh et al [1] investigating a SiC whisker reinforced 2124 alloy. At 525°C the elongation to failure was found to increase with increasing strain rate up to $3.3 \times 10^{-1} \text{s}^{-1}$. A relatively high strain rate sensitivity ($m=0.33$) was measured which corresponded to the highest elongation (300%). The term high strain rate superplasticity (HSRS) was used to describe this phenomenon. It has been suggested [2] that HSRS in MMCs is dominated by the presence of the reinforcement as composites produced with the matrices 2124, 7064 and 6061 were found to exhibit HSRS but the corresponding monolithic (unreinforced) matrix alloys were not. The presence of the reinforcement brings about three key microstructural changes: (i) refinement of the grain structure during thermomechanical processing, (ii) prevention of grain growth during superplastic forming and (iii) the introduction of many reinforcement/matrix interfaces.

Higashi [3] found the optimum strain rate for HSRS to increase as the grain size was reduced and most MMCs exhibiting HSRS [1,3-6] grain sizes are $3 \mu\text{m}$ and below. This is in agreement with the 2-3 μm grains of the current 7475 (17% reinforcement) MMC. Indeed, Mabuchi et al [4] and Zahid et al [7] suggested that a very fine grain structure is required for HSRS. Nieh and Wadsworth [8] observed 2124 and 7064 that exhibited HSRS only when reinforced and noted that the monolithic matrix alloys had much coarser grain structures than the composites. The high temperature deformation mechanisms e.g. slip, grain boundary sliding and diffusional creep are thought to be independent mechanisms and at any give temperature-stress-grain size combination the most easy to perform will dominate. The strain rate ($\dot{\epsilon}$) for grain boundary sliding exhibits a very strong grain size dependence and typically $\dot{\epsilon} \propto d^{-2}$ or $\dot{\epsilon} \propto d^{-3}$ where d is the grain size. Reduction of the grain size will therefore push the transition from grain boundary sliding to creep in the desired direction i.e. to higher strain rates. The relationship between strain rate and grain size in the superplastic region is given by [4]:

$$\dot{\epsilon} = A d^{-l} D \left(\frac{\sigma}{E} \right)^n$$

where D is the diffusivity, d is the grain size, σ is the stress, E is the elastic modulus, n is the stress exponent and l is the grain size dependence. It has been shown above that l is generally equal to 2-3. Therefore, according to the above equation reducing the grain size by a factor of two would be expected to increase the optimum strain rate for superplastic flow by a factor of 4-8 depending on the exact grain size relationship.

It can be seen from the forming envelope in Figure 3 and Table I that the highest angles of α are attained when forming is carried out above the matrix solidus (535°C). This is shown particularly well at 100psi where no step forms at 525°C but at 550°C a 35° step is formed. Higashi et al [9] noted that very fine grains are necessary for HSRS but is not the overriding factor as some very fine grained alloys do not exhibit HSRS. In their initial study Nieh et al [1] noted that fracture

surfaces at optimum superplasticity differed from those at room temperature. There was a large amount of whisker exposure (pull out) and the matrix did not exhibit well formed dimples but appeared to be less severely deformed and more granular. Other workers [6,10] have also noted filaments on final fracture surfaces at optimum superplasticity which is indicative of a liquid phase. They suggest that these filaments represent a partially melted matrix and that the processing is semi-solid. From Figure 6 it can be seen that filaments were exhibited on the fracture surface of the 7475 (17% reinforcement) material formed at 550°C in the current study. Imai et al [6] considered that the liquid phase allowed interfacial sliding between the matrix and reinforcement and this mechanism acted along side grain boundary sliding. Phar and Ashby [11] suggested that the liquid phases act as lubricants to facilitate particle and grain sliding.

It has been suggested that adiabatic heating and solute segregation that cause local melting [2,12] may be responsible for HSRS below the matrix solidus. However, the large improvement in formed angle α when forming above the matrix solidus and absence of filaments on the fracture surface of the material formed at 525°C (10°C below matrix solidus) suggests this is not the case in the current MMCs.

From the literature there appears to some disagreement as to whether fine grains [4,7] or the presence of a liquid phase [6,10] is responsible for HSRS. In the present study it should be noted that the 7475 (10% reinforcement) material split under forming even above the matrix solidus and did not exhibit HSRS; this material had coarser grains ($\sim 7 \times 15 \mu\text{m}$) compared to the 17% reinforced material (2-3 μm) which suggests that fine grains is the overriding factor in HSRS. Furthermore, HSRS was exhibited below the matrix solidus where no liquid phase was detected. However, it should be noted that above the matrix solidus where some liquid phase would be expected large improvements in step forming angle (12° at 200psi) were observed. Neih et al [13] stated that the fine grain structure is required as there will only be a small amount of liquid present ($\sim 5\%$). Due to the very fine grain size there is a high capillary force and only a small amount of liquid phase is required.

It is well known that cavity formation during superplastic forming can have a deleterious effect on the subsequent mechanical properties. Higashi and Mabuchi [5] believed that most cavities either pre-exist at the reinforcement or inclusions as a result of thermomechanical processing to achieve the superplastic microstructure or are generated by grain boundary sliding during superplastic forming due to too high an imposed deformation rate for the temperature and grain size. Optical microsections of the current materials (Figure 5) show no such cavitation and furthermore no back pressure was employed during forming. The likely reason for this is that the strain levels in the current study ($\sim 40\%$ across the step) are not high enough to cause cavitation. McDermid and Flitcroft [14] found that cavitation was not observed until strains of $\sim 100\%$ were exceeded in an 8090 MMC.

Conclusions

Steps were successfully superplastically formed in a 7475 MMC reinforced with 17vol% of 3 μm SiC particles. Strain rates measured ($\sim 2 \times 10^{-1} \text{s}^{-1}$) were found to be in the high strain rate region. Fine grain size was found to be more important for HSRS, however, large improvements in forming were observed above the matrix solidus where some liquid phase was present.

References

1. T.G. Nieh, C.A. Henshall and J. Wadsworth, *Scripta met. et mat.*, **18**, 1984, 1405.
2. T.G. Nieh and J. Wadsworth, *J.O.M.*, Nov., 1992, 46.
3. K. Higashi, *Mat. Sci. and Eng.*, **A166**, 1993, 109.
4. M. Mubachi, K. Higashi, Y. Okada, S. Tanimura, T. Imai and K. Kubo, *Scripta met. et mat.*, **25**, 1991, 2517.
5. K. Higashi and M. Mubachi, *Mat. Sci. and Eng.*, **A176**, 1994, 1739.
6. T. Imai, G.L'Esperance and B.D. Hong, *Scripta met. et mat.*, **31**, 1994, 321.
7. G.H. Zahid, R.I. Todd and P.B. Pragnell, *Proc. Conf. Metal Matrix CompositesVI*, The Royal Society, London, 1997.
8. T.G. Nieh and J. Wadsworth, *Mat. Sci. and Eng.*, **A147**, 1991, 129.
9. K. Higashi, T.G. Nieh and J. Wadsworth, *Acta Met. et Mat.*, **43**, 1995, 3275.
10. T.G. Nieh, T. Imai, J. Wadsworth and S. Kojima, *Scripta met. et mat.*, **31**, 1994, 1685.
11. G.M. Phar and M.F. Ashby, *Acta Met. et Mat.*, **31**, 1983, 129.
12. J. Kioke, M. Mabuchi and K. Higashi, *Acta Met. et Mat.*, **43**, 1995, 199.
13. T.G. Nieh, J. Wadsworth and T. Imai, *Scripta met. et mat.*, **26**, 1992, 703.
14. S.M. Flitcroft and D.S. McDarmid, Defence and Evaluation Research Agency, Technical Report, 92052, 1992.

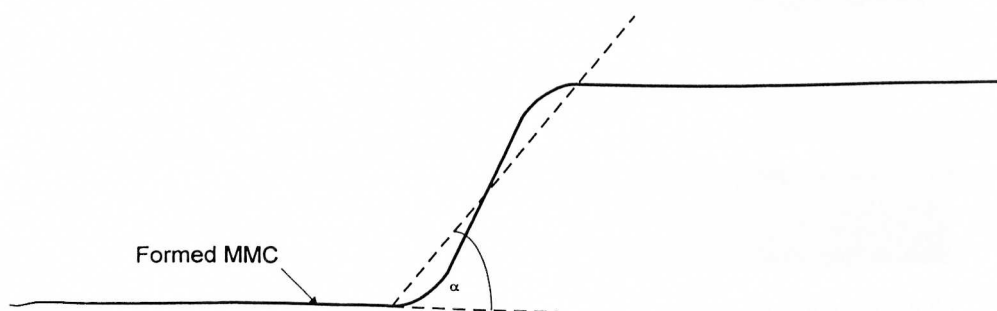


Figure 1. Measurement of angle formed in material

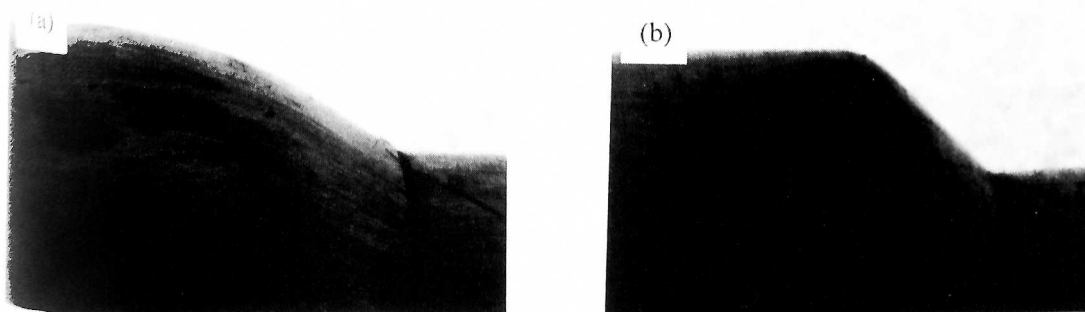


Figure 2. Photographs of steps formed in 17vol% material at (a) 450°C/300psi and (b) 550°C/200psi

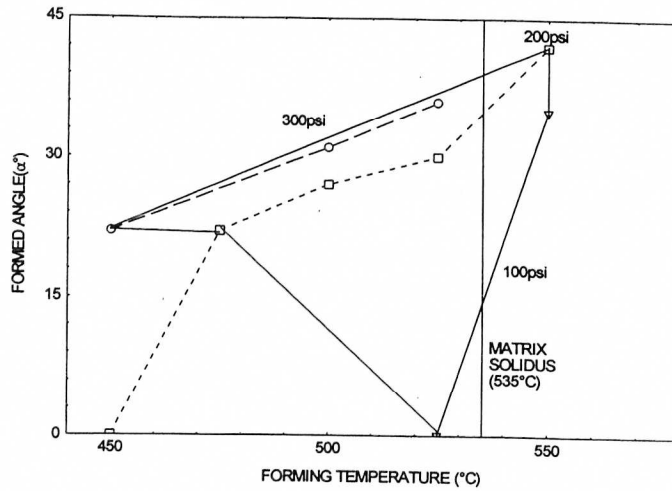


Figure 3. Forming envelope for the 17vol% reinforcement material

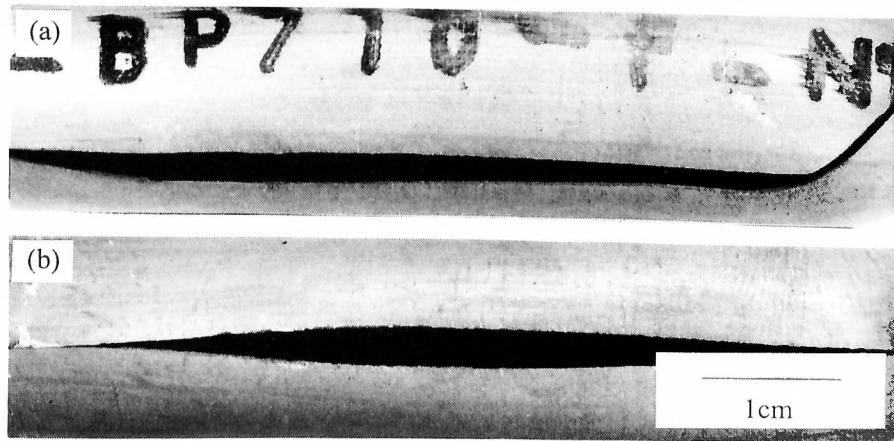


Figure 4. Photograph of splits in 10vol% material formed at (a) 525°C/300psi and (b) 550°C/200psi

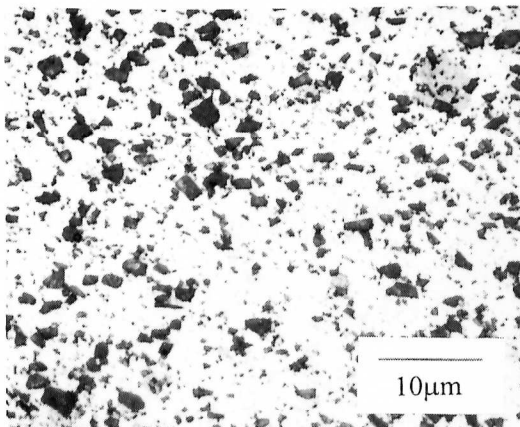


Figure 5. Optical micrograph of section through step region (17vol%)

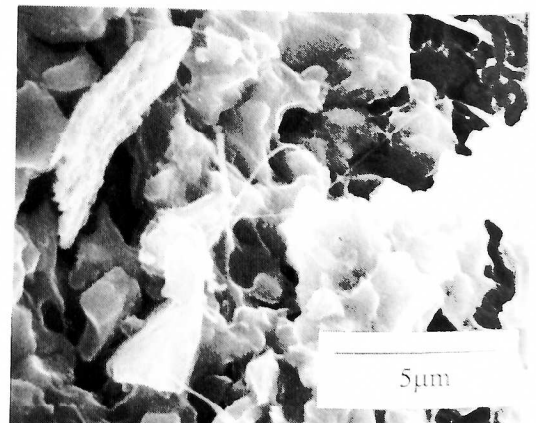


Figure 6. SEM micrograph of fracture surface (17vol%)